ACS APPLIED MATERIALS & INTERFACES

Research Article

www.acsami.org

Piezoresistance in Polymer Nanocomposites with High Aspect Ratio Particles

Cyrill Cattin and Pascal Hubert*

Structures and Composite Materials Laboratory, Department of Mechanical Engineering, McGill University, 817 Sherbrooke Street West, Montreal, Quebec H3A 0C3, Canada

ABSTRACT: In this paper, we address the problem of positive piezoresistance in high aspect ratio particle based polymer nanocomposites, a hybrid system at the center of research on flexible piezoresistive materials. We introduce a percolation theory based model relating the variation in electrical resistance to compressive strain and show that it gives accurate theoretical fits to experimental data presented in this paper, as well as to much of the available data in the literature. In contrast to existing theories, the model captures the characteristics of the particle network through experimentally definable parameters and does not rely on assumptions regarding the nature of the particles and/or the configuration of the network. It is further demonstrated that the presented theoretical framework is not limited to polymer nanocomposites with high aspect ratio particle but that it can explain piezoresistance in bulk electroconductive polymer nanocomposites in general. We find that the piezoresistive effect in such materials is rooted in a mechanical deformation induced change in the distribution of local conductances within the particle network, and we show that this change in the distribution of local conductances is well described by a strain dependent conductivity exponent, which scales with the magnitude of mechanical deformation. Besides, we demonstrate that these findings can be applied to the experimentally observed concentration dependence of the piezoresistance in polymer nanocomposites and, thus, to predicting the electric response to mechanical deformation at any particle concentration, which is expected to be highly instrumental in applied materials selection and performance evaluation.

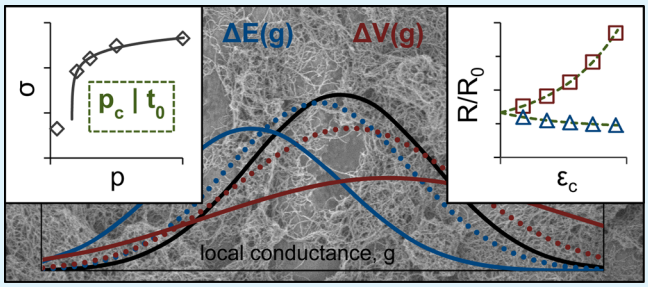

KEYWORDS: *piezoresistance, nanocomposites, functional polymer composites, sensing, modeling*

1. INTRODUCTION

Adding electrically conducting nanoparticles to polymers allows for the design of electroconductive polymer nanocomposites, where electron flow is enabled through the formation of a particle network throughout the polymer matrix.[1,2] The characteristics of the particle network (e.g., the mean interparticle separation) and, consequently, the overall electrical resistance of the material change with mechanical deformation, making such nanocomposites piezoresistive materials.[3−29] Electroconductive polymer nanocomposites are therefore an interesting candidate for applications as functional materials, where polymers are preferred to metals or ceramics but where electrical conductivity and piezoresistance are required material properties as, for example, in flexible tactile sensors.[30]

Uniaxial tension on bulk electroconductive polymer nanocomposites generally leads to an increase in electrical resistance,[3−13] whereas the electric response to uniaxial compression seems to depend on particle shape: the electrical resistance typically decreases with compressive strain in the case of low aspect ratio particles (e.g., low structure carbon black and metal powder)[14−19] but increases with compressive strain in the case of high aspect ratio particles (e.g., high structure carbon black agglomerates, carbon nanotubes, and graphite nanosheets).[3,20−29] In either case, the piezoresistance strongly depends on particle concentration and increases with decreasing particle content.[7,8,17,18,23,25−27] The determinant for the overall electrical resistance in electroconductive polymer nanocomposites is the contact resistance between neighboring particles within the conducting network, which in turn, is dominated by quantum mechanical tunneling through insulating polymer layers,[31,32] and so is a function of interparticle separation. Accordingly, the positive interdependence of electrical resistance and uniaxial tension, as well as the negative interdependence of electrical resistance and uniaxial compression, can be explained with the change in mean interparticle separation: as the particle network is stretched, the overall electrical resistance increases because the mean interparticle separation is increased, and as the particle network is compressed the overall electrical resistance decreases because the mean interparticle separation is decreased. In both cases, the experimentally observed piezoresistance is found to be well described by models based on quantum mechanical tunneling or thermal activation over barriers.[3,6,9,10,15,17,18] Such modeling, however, involves nontrivial parameters, namely, the height of

Received: October 29, 2013
Accepted: January 10, 2014
Published: January 10, 2014

   dx.doi.org/10.1021/am404808u | ACS Appl. Mater. Interfaces 2014, 6, 1804−1811

the tunneling potential barrier and the average initial interparticle separation, and generally is concentration specific, hence inapplicable to predicting the experimentally observed concentration dependence of the piezoresistance.

In contrast to the above, the positive interdependence of electrical resistance and uniaxial compression, as it is found in polymer nanocomposites with high aspect ratio particles, is not well understood. An increase in interparticle separation with uniaxial compression of the particle network, i.e., as the occupied volume is reduced, seems unobvious. Oliva-Aviles et al.[33] have investigated the contribution of carbon nanotube (CNT) deformation to the piezoresistance of a CNT−polymer nanocomposite and found that it is marginal and that the overall electric response to mechanical deformation is dominated by changes in the configuration of the CNT network. Accordingly, by considering the electrical resistance of the conducting particles as constant, it has been proposed that the piezoresistance in polymer nanocomposites with high aspect ratio particles can be explained by a combination of two distinct mechanisms, namely, a change in interparticle separation, as discussed in the previous paragraph, and a change in the number of conducting paths within the particle network.[15,23,25,27] Quantum mechanical tunneling based models, that have been extended to account for such changes in the number of conducting paths, were found to fit the electric response to uniaxial compression in well-defined systems;[23,25] they remain, however, concentration specific and are not generally applicable.

In electroconductive polymer nanocomposites, the percolation threshold, i.e., the minimum particle concentration needed to form an electron-conducting network throughout the polymer matrix, is inversely proportional to the aspect ratio of the particles.[34,35] With regard to applications as functional materials where the polymeric characteristics of the material, e.g., transparency and/or flexibility, are key requirements, high aspect ratio particle based polymer nanocomposites are therefore of particular interest, as the added properties, i.e., electrical conductivity and piezoresistance, can be obtained at much lower particle content. Thence, there is a clear need for a better understanding of the piezoresistance in such materials. Moreover, as mentioned before, the piezoresistance of electroconductive polymer nanocomposites is tunable because it is concentration dependent. Having the capacity to predict this concentration dependence of the piezoresistance would be highly instrumental in the selection of functional materials for piezoresistive sensing applications. In this paper, we present a new theoretical framework for a general understanding of the piezoresistive effect in polymer nanocomposites. First, we address the problem of positive piezoresistance in polymer nanocomposites with high aspect ratio particles. We introduce a model relating the particle concentration dependent variation in electrical resistance to compressive strain and apply it to our electromechanical characterization of a CNT based polymer nanocomposite, as well as to related data from the literature on CNT, graphene, and high structure carbon black based polymer nanocomposites. With the aim of contributing to a general understanding of piezoresistance in polymer nanocomposites, we then show why current theories fail to generally describe the experimental findings and discuss the electric response to compressive and tensile deformation of both high aspect ratio particle and low aspect ratio particle based polymer nanocomposites.

2. THEORETICAL BASIS AND MODEL

The overall electrical conductance, G, of an electroconductive polymer nanocomposite scales positively with the fractional particle content, p, and for $p > p_c$ typically follows the power-law behavior:

$$G \propto (p - p_c)^t \tag{1}$$

where p_c is the percolation threshold, i.e., the particle concentration below which G vanishes, and t is the so-called conductivity exponent. For the case of direct contact between adjacent particles, classical percolation theory predicts the conductivity exponent to be universal, i.e., not dependent upon the nature of the particles and the configuration of the network, and solely dependent on the network dimensionality (e.g., $t = 2$ for all three-dimensional direct-contact networks).[36] By fitting eq 1 to experimental results, many bulk electroconductive polymer nanocomposites, however, are found to be characterized by nonuniversal conductivity exponents.[35,37] Studying this discrepancy between experimental data and available theories, Balberg proposed a tunneling-percolation model,[38] in which electron conduction through the percolating network is dominated by tunneling between adjacent but noncontacting particles and identified quantum mechanical tunneling as the potential origin of this nonuniversality. Experimental evidence for a determinant role of quantum mechanical tunneling is found in both polymer nanocomposites with low aspect ratio particles[31] and polymer nanocomposites with high aspect ratio particles,[32] and on the basis of Balberg's work, it is now understood that the magnitude of the deviation from the universal value of t is governed by the distribution of local conductances.[39−42]

The tunneling probability and, so, the local conductance depend exponentially on interparticle separation. It therefore seems likely that, due to reorientation, reshaping, and relative movement of the particles, uniaxial compression of a polymer nanocomposite with high aspect ratio particles will affect the local conductances, such that part of it increases, part of it remains unchanged, and part of it decreases, leading to a net broadening of the distribution of local conductances. Recently, Scardaci et al.[43] found the conductivity exponent of a high aspect ratio particle based polymer nanocomposite to scale linearly with network nonuniformity, suggesting higher t values for broader distributions of local conductances. Accordingly, we assume that uniaxially compressed bulk polymer nanocomposites with high aspect ratio particles are characterized by an increased conductivity exponent; hence, that t scales positively with applied compressive strain, ε_c. We therefore propose that t can be replaced by a compressive strain dependent conductivity exponent, t_c:

$$t_c(\varepsilon_c) = t_0(1 + c_p|\varepsilon_c|) \tag{2}$$

where $0 \leq |\varepsilon_c| \leq 1$, t_0 is the reference conductivity exponent characterizing the particle network at compressive strain ε_0 (typically $\varepsilon_0 = 0$), and c_p is a factor taking into account the concentration dependence of the influence of compressive strain on the distribution of local conductances. By inverting eq 1 and replacing t by t_c given in eq 2, one so obtains an expression for the compressive strain dependent overall electrical resistance of the material, R_c:

$$R_c(\varepsilon_c) \propto (p - p_c)^{-t_0(1+c_p|\varepsilon_c|)} \tag{3}$$

As discussed before, the piezoresistance in polymer nanocomposites is concentration dependent and increases with decreasing particle content. We therefore assume that the influence of ε_c on the distribution of local conductances decreases as the number of local conductors, i.e., two particles within the electron conducting network close enough to allow for quantum mechanical tunneling, increases; thence as the particle concentration increases, it is highest at p close to p_c and decreases as $(p - p_c)$ increases. A simple expression for this is given by:

$$c_p = \frac{p_c}{p} \tag{4}$$

Thus, by substituting the above expression in eq 3 and normalizing $R_c(\varepsilon_c)$ to the reference electrical resistance at ε_0, $R_c(\varepsilon_0)$, the variation in normalized electrical resistance with uniaxial compression of a polymer nanocomposite with high aspect ratio particles, i.e., its piezoresistance, can conveniently be described as:

$$\frac{R_c(\varepsilon_c)}{R_c(\varepsilon_0)} = (p - p_c)^{t_0 \frac{p_c}{p}(|\varepsilon_0| - |\varepsilon_c|)} \tag{5}$$

Prominent features of this model are that it captures the concentration dependence of the piezoresistance and that no assumptions need to be made with respect to the nature of the particles and/or the configuration of the network, as both of them are described by parameters p_c and t_0, which are experimentally definable.

3. RESULTS AND DISCUSSION

First, provided p_c and t_0 are known, eq 5 enables one to evaluate the piezoresistance at any particle concentration of $p > p_c$. Second, given that parameters p_c and t_0 are specific to a particle network, eq 5 should apply to any uniaxially compressed polymer nanocomposite with high aspect ratio particles. The underlying assumptions are that the particle network at ε_0 is indeed well characterized by the parameters p_c and t_0 and that the evolution of the characteristics of the particle network and, consequently, of the overall electrical resistance of the material is captured by the strain dependence of the conductivity exponent. Next, we study the first point by applying eq 5 to our electromechanical characterization of a high aspect ratio particle based polymer nanocomposite, where we experimentally define parameters p_c and t_0, and study the fit of the model at different particle concentrations. We then verify the second point by applying our model to appropriate data from the literature on various polymer nanocomposites.

3.1. Predicting the Concentration Dependence of the Piezoresistance. The high aspect ratio particle based electroconductive polymer nanocomposite studied herein is a multiwalled carbon nanotube (MWCNT) modified polydimethylsiloxane (PDMS). Figure 1 shows the electrical conductivity, σ, of the MWCNT−PDMS nanocomposite at eight different CNT mass fractions (empty symbols). As expected, the electrical conductivity scales positively with CNT concentration, showing a sudden transition from a nonconducting to a conducting regime, with a relatively moderate increase at high CNT content. Parameters p_c and t_0 of eq 5, characterizing the MWCNT network throughout the PDMS matrix at ε_0, are obtained by means of a logarithmic plot of σ vs $(p - p_c)$ (cf. inset in Figure 1) where p_c is incrementally varied until the best linear fit of eq 1 to the experimental data is obtained. Note that the power-law behavior in eq 1 also applies to the electrical conductivity, σ, and that G is replaced by σ. For the system at hand, the parameters were found to be $p_c \approx 0.00325$ and $t_0 \approx 2.8$, respectively, with a coefficient of determination of 0.99232. The proportionality constant, σ_0, used to fit eq 1 to the semilogarithmic plot of σ vs p (solid line), which was also obtained through the fitting procedure, was $\sigma_0 \approx 2.2 \times 10^3$ S/m.

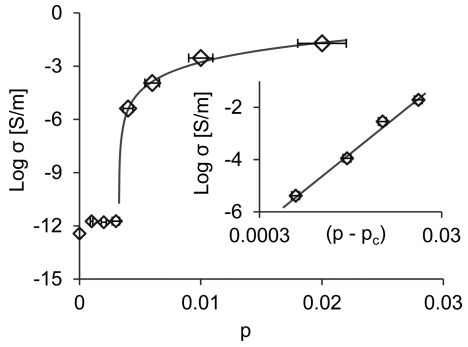

Figure 1. Semilogarithmic plot of measured (empty symbols) and calculated (solid line) change in electrical conductivity, σ, with MWCNT mass fraction, p. Reported σ values for $p \leq 0.003$ were obtained according to ASTM D257, and σ values for $p \geq 0.004$ were obtained on cube samples at the reference point, i.e., at $\varepsilon_0 = 0.11$, taking into account the corresponding sample dimensions. Inset: logarithmic plot of σ vs $(p - p_c)$ showing the best fit of eq 1 to the experimental data.

The measured electric response to uniaxial compression of the MWCNT−PDMS nanocomposite is shown in Figure 2a (empty symbols), for a CNT mass fraction close to the percolation threshold, i.e., 0.004, and a high CNT mass fraction, i.e., 0.01, as well as one in between, i.e., 0.006. In line with data reported for other high aspect ratio particle based bulk polymer nanocomposites, first, the electrical resistance increases with compressive strain and, second, the interdependence of electrical resistance and compressive strain is exponential in type and shows a particle concentration dependent behavior, with increasing strain-sensitivity for decreasing particle content. Figure 2a also shows the calculated electric response to uniaxial compression as obtained by eq 5 for the same CNT mass fractions (solid lines), using the previously determined values for parameters p_c and t_0. It appears that both the piezoresistance of the MWCNT−PDMS nanocomposite as well as its concentration dependence are well described by the proposed model, indicating that the electric response to uniaxial compression is indeed dominated by a net broadening of the distribution of local conductances and that the influence of compressive strain on this distribution is inversely proportional to particle concentration. Although other expressions for c_p cannot be ruled out, the goodness of the fit further indicates that this interdependence is well captured by the simple expression given in eq 4. Analyzing the σ vs $(p - p_c)$ trends at different compressive strains (cf. Figure 2b), the conductivity exponent (slope of the linear fits to the experimental data) is found to increase with increasing compressive strain, which confirms the corresponding assumption made leading up to eq 2 (i.e., that t scales positively with ε_c).

Given the dependence of $t_c(\varepsilon_c)$ on p_c and t_0 (cf. eqs 2 and 4), it is worth noting that both p_c and t_0 are considered strain independent. Parameters p_c and t_0 characterize the particle network at the reference point ε_0 and, for a given p, $t_c(\varepsilon_c)$ then

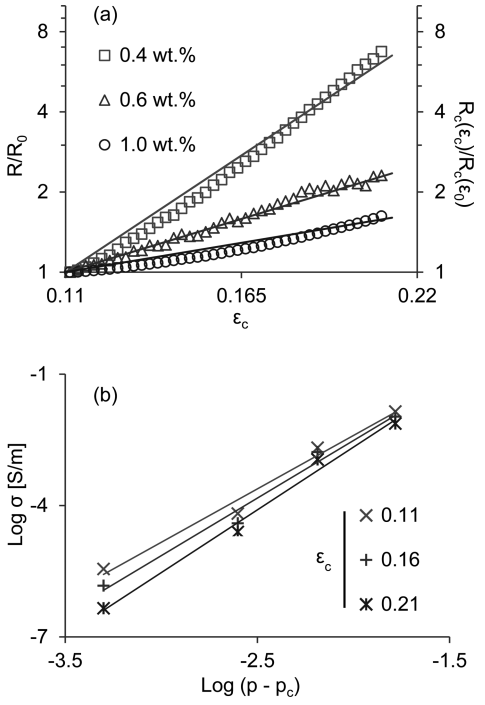

Figure 2. (a) Semilogarithmic plot of variation in normalized electrical resistance, R/R_0, with uniaxial compression, ε_c, of the MWCNT−PDMS nanocomposite at three CNT mass fractions (empty symbols), R_0 being the resistance measured at $\varepsilon_0 = 0.11$, and calculated electric response, $R_c(\varepsilon_c)/R_c(\varepsilon_0)$, to uniaxial compression, as obtained by eq 5 for the same CNT mass fractions (solid lines). (b) Logarithmic plot of σ vs $(p - p_c)$ showing the linear fits (solid lines) to the experimental data (line symbols) at three different compressive strains ε_c.

captures the change in the distribution of local conductances with compressive strain $|\varepsilon_c| \geq |\varepsilon_0|$. Parameters p_c and t_0 are a function of constituent materials, processing method and reference point (e.g., precompression); a change of any of those parameters would likely lead to different p_c and t_0 values.

3.2. Applying the Model to Data from the Literature.

For the purpose of applying our model to different polymer nanocomposites, we have identified a number of papers that study the electric response to uniaxial compression of bulk polymer nanocomposites with high aspect ratio particles, namely, refs 3, 22, 24−26, 28, and 29. The extracted data for seven CNT, graphene, and high structure carbon black based polymer nanocomposites are shown in a R/R_0 vs ε_c plot in Figure 3 (full and empty symbols). In case the electric response was given as a function of pressure or compressive force, the corresponding compressive strain was derived by taking into account the Young's modulus, Y, of the material, as is described in the Materials and Methods section. For the same polymer nanocomposites, Figure 3 also shows the calculated electric response to uniaxial compression as obtained by eq 5 (solid and dashed lines), using the respective parameters listed in Table 1.

First of all, in spite of the large range of variations in relative resistance, the piezoresistance of all seven polymer nanocomposites is well characterized by our model. The model was applied to data from ref 25, by using the p, p_c, and t_0 values given in the paper and incrementally changing Y until the best fit was obtained. The so found values for the Young's modulus of the material seem reasonable, and higher Y values were found for higher CNT concentrations, as is expected for MWCNT−methylvinyl silicone rubber (VMQ) nanocomposites. In both systems, i.e., for MWCNT−VMQ nanocomposites with CNTs having an average aspect ratio of around 50 (data sets 1 and 2) as well as for MWCNT−VMQ nanocomposites with CNTs having an average aspect ratio of around 500 (data sets 3 and 4), eq 5 also captures well the concentration dependence of the piezoresistance. To fit eq 5 to data from ref 28, values for p and p_c were taken from the paper; an assumption for Y was made based on data from the material supplier, and t_0 was the fitting parameter. Again, the so obtained value falls within the expected range. Given the difference in MWCNT aspect ratio for the polymer nanocomposites presented in ref 25 (e.g., data sets 1 and 3) and the fact that the polymer nanocomposite characterized in ref 28 (data set 5) is composed of modified MWCNTs and a different matrix material, it seems self-evident that the corresponding CNT networks at $\varepsilon_0 = 0$ differ from each other. The equally good fits of eq 5 to data sets 1, 3, and 5, for different respective sets of p_c and t_0 values (cf. Table 1), therefore strongly support the assumptions that the particle network at ε_0 is well characterized by the corresponding p_c and t_0 values and that the variation in electrical resistance with uniaxial compression is indeed captured by the strain dependence of the conductivity exponent.

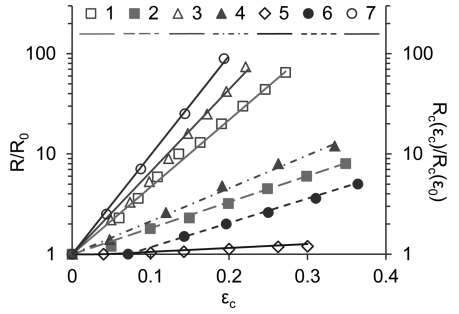

Figure 3. Semilogarithmic plot of variation in normalized electrical resistance, R/R_0, with uniaxial compression, ε_c, for seven high aspect ratio particle based polymer nanocomposites (full and empty symbols) and the corresponding calculated electric response, $R_c(\varepsilon_c)/R_c(\varepsilon_0)$, to uniaxial compression as obtained by eq 5 (solid and dashed lines). Data sources and parameters p, p_c, t_0, and Y are specified in Table 1. For improved facility of inspection, ε_c values of data set 5 were multiplied by 10.

In ref 25, a higher percolation threshold was found for the nanocomposite with the higher aspect ratio CNTs. This is unusual as, typically, the percolation threshold is inversely proportional to the particle aspect ratio.[34,35] The authors explain this discrepancy with the agglomeration of CNTs, which decreases the effective aspect ratio and appears to be more pronounced for the higher aspect ratio ones. It is worth noting that, despite this discrepancy, eq 5 describes data sets 1 to 4 equally well. The reason for this is that the description of the respective CNT networks is based on experimentally defined parameters and does not rely on assumptions regarding particle geometry and/or network configuration and that eq 5 is equally applicable to networks of well-dispersed particles and networks comprising particle agglomerates. Same as for data sets 1 to 4, eq 5 was applied to the graphene−PDMS nanocomposite (data set 6) by using the p, p_c, and t_0 values given in the corresponding paper and incrementally changing Y until the best fit was obtained. For the high structure carbon black−polyisoprene (PI) nanocomposite (data set 7), an estimation of p_c is given by the same authors in ref 5; Y was

Table 1. Parameters p, p_c, t_0, and Y Used to Fit Eq 5 to Data from the Literature (cf. Figure 3)

label	ref	constituent materials	comment	p	p_c	t_0	Y [MPa]
1	25	MWCNT − VMQ	CNT aspect ratio: 50	0.011	0.0082	3.52	6.5[b]
2				0.021			7.1[b]
3	25	MWCNT − VMQ	CNT aspect ratio: 500	0.013	0.0102	4.16	7.2[b]
4				0.025			7.4[b]
5	28	MWCNT − PDMS	modified CNTs	0.01	0.0075	2.3[b]	4[a]
6	29	graphene − PDMS	−	0.0119	0.0063	2.12	1.4[b]
7	3	high structure NCB[c] − PI	−	0.1	0.09[a]	5.5[b]	0.4[a]

[a]Estimated value. [b]Fitting parameter. [c]Nanosized carbon black.

estimated on the basis of data reported in literature,[44] and t_0 was the fitting parameter. In both cases, the so obtained values lie within the expected range, and the piezoresistance is well characterized by our model. This suggests that the notion of a net broadening of the distribution of local conductances with compressive strain applies to all high aspect ratio particle based polymer nanocomposites. We therefore conclude that eq 5 can indeed be universally applied to bulk polymer nanocomposites with high aspect ratio particles. It is worth noting that the piezoresistances of the polymer nanocomposites studied in refs 22, 24, and 26 are equally well described by eq 5; data from these three references was not included in Figure 3, though, to avoid a loss of clearness.

3.3. Understanding Piezoresistance in Bulk Polymer Nanocomposites. To conclude, we attempt to demonstrate that the framework of the proposed model is not limited to high aspect ratio particle based polymer nanocomposites but that it can describe piezoresistance in electroconductive polymer nanocomposites in general. To this end, we assume that the dispersion of the particles within the polymer matrix is such that the local conductances, g, follow some distribution around a mean value. The overall electrical conductance, G, of a bulk polymer nanocomposite is then a function of both the mean local conductance, $E(g)$, and the variance of this distribution of local conductances, $V(g)$. On the one hand, for a given $V(g)$, G increases with increasing $E(g)$, i.e., decreasing mean interparticle separation, and decreases with decreasing $E(g)$, i.e., increasing mean interparticle separation. On the other hand, for a given $E(g)$, G increases with decreasing $V(g)$ and decreases with increasing $V(g)$. The reason for this is that the range of g is finite, with a maximum in the case of physical contact between particles and a minimum in the case of high interparticle separation, where the corresponding particle−particle junction can no longer be considered as a conductor.

Upon mechanical deformation, $E(g)$ is increased or decreased, depending on whether the particle network is compressed or stretched. $V(g)$, in contrast, is always increased. To illustrate this, we discuss a case of uniaxial compression, as is schematically shown in Figure 4. On the one hand, as the bulk polymer nanocomposite is compressed, the overall volume occupied by the particle network is reduced and so is the mean interparticle separation, with the consequence that $E(g)$ is increased. On the other hand, upon compression, the distance between two adjacent particles either decreases (cf. mode 1 in Figure 4) or increases (cf. mode 2 in Figure 4) or remains unchanged (mode 0, not shown in Figure 4), depending on the details of this individual particle−particle junction (e.g., orientation with respect to the direction of the applied compressive load or position within the particle network). The probability of occurrence for the three modes is typically

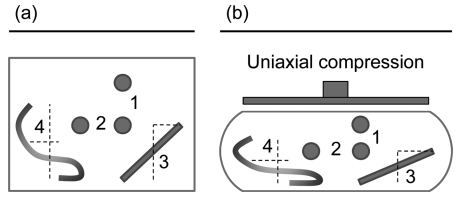

Figure 4. Schematic, two-dimensional representation of interparticle distances (a) prior to and (b) after uniaxial compression of an unconstrained bulk polymer nanocomposite. The changes are due to, first, relative movement of the particles (modes 1 and 2) and, second, reorientation and reshaping of the particles (modes 3 and 4).

not equal. However, because the probability of occurrence for the three modes is typically independent of the interparticle separation at ε_0, the probability for an increase in g is therefore equal for all g, as is the probability for a decrease in g or a zero-change. Consequently, as the number of particle−particle junctions for which $g = g_i$ is highest for $g_i = E(g)$ and lower for $g_i < E(g)$ and $g_i > E(g)$, the compression of the particle network results in a net broadening of the distribution of local conductances and, hence, an increase in $V(g)$. From this follows that in the case of uniaxial compression of bulk polymer nanocomposites, the overall electrical resistance, $R = 1/G$, can increase or decrease, because the increase of $E(g)$ and the increase of $V(g)$ have opposite effects on R (i.e., because R scales with $V(g)$ but with the inverse of $E(g)$), whereas in the case of uniaxial tension, R increases because $E(g)$ decreases and $V(g)$ increases. This is in good agreement with experimental evidence, as the interdependence of electrical resistance and mechanical deformation can be positive or negative in the case of uniaxial compression[3,14−29] but is generally positive in the case of uniaxial tension.[3−13]

The fact that the electrical resistance typically decreases with uniaxial compression of low aspect ratio particle based polymer nanocomposites[14−19] but increases with uniaxial compression of high aspect ratio particle based polymer nanocomposites[3,20−29] suggests that in the first case the electric response is dominated by the change in $E(g)$, $\Delta E(g)$, whereas in the second case, it is the change in $V(g)$, $\Delta V(g)$, that dominates the electric response. This can be understood by looking at the nanoscale mechanisms that lead to a change in the distribution of local conductances. In low aspect ratio particle based polymer nanocomposites, the change in the distribution of local conductances due to mechanical deformation of the particle network is caused by relative movement of particles (cf. modes 1 and 2 in Figure 4). In this case, for a given deformation, $\Delta V(g)$ is inversely proportional to $\Delta E(g)$ (e.g., $\Delta V(g)$ is at a maximum in the case of equal and nonzero probabilities for the distances between adjacent particles to increase or decrease, in which case $\Delta E(g) = 0$). As $\Delta E(g)$ typically is nonzero, $\Delta V(g)$ is

reduced accordingly and it appears to be likely that the electric response is then dominated by $\Delta E(g)$. In high aspect ratio particle based polymer nanocomposites, in contrast, the distribution of local conductances within the particle network is affected not only through relative movement of the particles but also through reorientation and reshaping of the particles (cf. modes 3 and 4 in Figure 4). We believe that particle reorientation and reshaping is a more random process, with closer probabilities for the distances between adjacent particles to increase or decrease, which consequently, for the same mechanical deformation, leads to smaller $\Delta E(g)$ and larger $\Delta V(g)$, such that $\Delta V(g)$ dominates the electric response.

From the above, it follows that electroconductive polymer nanocomposites are piezoresistive materials because the distribution of local conductances within the particle network changes with mechanical deformation of the latter and that this change in distribution of local conductances is described with $\Delta E(g)$ and $\Delta V(g)$. Models based on quantum mechanical tunneling or thermal activation over barriers have in common that the change in R with deformation is given as a function of the change in mean interparticle separation. Thence, such modeling considers the influence of $\Delta E(g)$ on the electric response but ignores the effect of $\Delta V(g)$. In the case of uniaxial tension, qualitatively good fits are obtained because the effects of $\Delta E(g)$ and $\Delta V(g)$ on R are similar in type, and neglecting the effect of $\Delta V(g)$ does not change the general trend. Similarly, in the case of uniaxial compression of low aspect ratio particle based polymer nanocomposites, qualitatively good fits are obtained because the electric response is dominated by $\Delta E(g)$. In the case of high aspect ratio particle based polymer nanocomposites, however, where the electric response is dominated by $\Delta V(g)$, such modeling fails to describe the experimental findings.

The model presented in this paper considers the influences of both $\Delta E(g)$ and $\Delta V(g)$. The influence of $\Delta V(g)$ is accounted for by considering a positive interdependence of t and ε_c, and the influence of $\Delta E(g)$ is factored in by considering the strain dependence of the conductivity exponent in the first place. Note that eq 5 can be rewritten as:

$$\frac{R_c(\varepsilon_c)}{R_c(\varepsilon_0)} = (p - p_c)^{t_0\frac{p}{p_c}(|\varepsilon_0|-|\varepsilon_c|)} = e^{t_0\frac{p}{p_c}\ln(p-p_c)(|\varepsilon_0|-|\varepsilon_c|)} \quad (6)$$

where in the second equality it is made explicit that the interdependence of R_c and ε_c is exponential in type, as it is expected for percolated networks where electron conduction is dominated by tunneling between adjacent but noncontacting particles and where the mean interparticle separation and, hence, $E(g)$, is a function of applied strain. Our model might therefore be generalized to describe the electric response to mechanical deformation of bulk polymer nanocomposite in general. Such a generalized relation between the overall electric resistance, $R(\varepsilon)$, and the applied strain, ε, might be given by:

$$\frac{R(\varepsilon)}{R(\varepsilon_0)} = (p - p_c)^{(1-\theta(\alpha)\xi(\varepsilon))t_0 c_p(|\varepsilon_0|-|\varepsilon|)} \quad (7)$$

where $R(\varepsilon_0)$ is the reference resistance at strain ε_0, α is the de facto aspect ratio of the particles or agglomerates, $\theta(\alpha) = 2$ for $\alpha \approx 1$ and $\theta(\alpha) = 0$ for $\alpha \gg 1$, and $\xi(\varepsilon) = 1$ for $\varepsilon < 0$ and $\xi(\varepsilon) = 0$ for $\varepsilon > 0$. In Figure 5, we have applied eq 7 to appropriate data from the literature on uniaxially compressed bulk polymer nanocomposites with low aspect ratio particles, on the one hand, and on uniaxially stretched bulk polymer nanocomposites with both low and high aspect ratio particles on the other hand. Equation 4 was used to calculate c_p, and all other parameters are listed in Table 2.

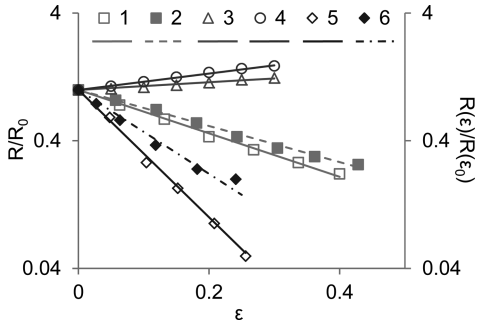

Figure 5. Semilogarithmic plot of measured variation in normalized electrical resistance, R/R_0, (full and empty symbols), and corresponding calculation, $R(\varepsilon)/R(\varepsilon_0)$, as obtained by eq 7 (dashed and solid lines), for the uniaxial compression of four low aspect ratio particle based polymer nanocomposites (squares and diamonds) and the uniaxial tension on both a low aspect ratio particle (triangles) and a high aspect ratio particle (circles) based polymer nanocomposite. Data sources and parameters $\theta(\alpha)$, $\xi(\varepsilon)$, p, p_c, t_0, and Y are specified in Table 2. For improved facility of inspection, ε values of data sets 3 and 4 were multiplied by 10.

It appears that the electric response to mechanical deformation in all six examples is well described by eq 7. This illustrates that piezoresistance in polymer nanocomposites in general can indeed be understood in terms of a change in the distribution of local conductances, which is characterized by $\Delta E(g)$ and $\Delta V(g)$, and well described by a deformation dependent conductivity exponent, which scales positively with applied strain. This applies to different polymer nanocomposites as well as to different particle concentrations for a given material system (cf. fits to data sets 1 and 2 in Figure 5).

4. SUMMARY AND CONCLUSIONS

High aspect ratio particle based polymer nanocomposites are at the center of research on flexible piezoresistive materials. The electric response to uniaxial compression of such materials is tunable because it is concentration dependent and can be highly sensitive because it is exponential in type. Whereas in low aspect ratio particle based polymer nanocomposite the experimentally found negative piezoresistance can generally be well explained with the corresponding decrease in mean interparticle separation, the experimentally observed positive piezoresistance in high aspect ratio particle based polymer nanocomposites is not yet well understood.

In this paper, we have addressed this problem theoretically and experimentally. By considering the conductivity exponent to be strain dependent and, therefore, to scale with the change in distribution of local conductances, we have developed a percolation theory based model, which relates the variation in electrical resistance of bulk polymer nanocomposites with high aspect ratio particles to compressive strain. The model captures the characteristics of the particle network through the experimentally definable percolation threshold, p_c, and reference conductivity exponent, t_0, and does not rely on assumptions regarding the nature of the particles and/or the configuration of the network.

We have shown that the model fits extremely well to experimental data for carbon nanotube, graphene, and high structure carbon black based polymer nanocomposites and

Table 2. Parameters $\theta(\alpha)$, $\xi(\varepsilon)$, p, p_c, t_0, and Y Used to Fit Eq 7 to Data from the Literature (cf. Figure 5)

label	ref	constituent materials	$\theta(\alpha)$	$\xi(\varepsilon)$	p	p_c	t_0	Y [MPa]
1	17	NCB[c] − polyethylene	2	1	0.25	0.15[a]	3.2[a]	95[b]
2					0.30			105[b]
3	10	NCB[c] − epoxy	2	0	0.005	0.0025[a]	2.3[b]	–
4		MWCNT − epoxy	0	0	0.003	0.002[a]	3.2[b]	–
5	17	Sn/Pb[d] − polyethylene	2	1	0.30	0.25[a]	4.4[b]	125[a]
6	14	SnO_2:Sb[e] − f -poxy[f]	2	1	0.244	0.21	2.6[b]	55[a]

[a]Estimated value. [b]Fitting parameter. [c]Nanosized carbon black. [d]Nanosized tin/lead alloy powder. [e]Nanosized antimony-doped tin oxide powder. [f]Flexible epoxy resin.

therefore conclude that it is universally applicable to high aspect ratio particle based polymer nanocomposites. Accordingly, we believe that the electric response to uniaxial compression of such materials is dominated by a net broadening of the distribution of local conductances, which in turn, is caused by reorientation, reshaping, and relative movement of the particles. We have further shown that piezoresistance in polymer nanocomposites in general can be understood in terms of a change in the distribution of local conductances. Both the mean local conductance and the variance of the distribution of local conductances are well described by the strain dependent conductivity exponent, which scales with the magnitude of applied mechanical deformation.

By applying the model to the electromechanical characterization of MWCNT−PDMS nanocomposites with varying MWCNT content, we have also shown that the concentration dependence of the piezoresistance in such materials is well captured by the proposed model. Provided parameters p_c and t_0 are known, it therefore allows for one to predict the piezoresistance at any particle concentration above the percolation threshold. With regard to piezoresistive sensing applications with set key requirements for the functional material (e.g., flexibility, transparency, dimensions, operating voltage/current, applied pressure, and/or required sensitivity), we believe that the model demonstrated in this paper will be instrumental in material selection and performance evaluation.

5. MATERIALS AND METHODS

5.1. Materials and Sample Preparation. PDMS (Gelest OE41) was purchased from Gelest, Inc., and MWCNTs (Baytubes C 150 P) were obtained from Bayer MaterialScience LLC. Toluene was used as an organic solvent to facilitate MWCNT deagglomeration and mixing of the constituent materials. For each concentration, the desired amount of MWCNTs was first dispersed in toluene for 90 min, using an ultrasonic bath (Model 2510, Branson Ultrasonics Corp.), and then added to the PDMS base polymer and the PDMS curing agent, such that the MWCNT/toluene to PDMS weight ratio was 1:3. Subsequently, the mixture was shear-mixed for 5 min, using a disperser (T 10 basic Ultra-Turrax, IKA Works, Inc.) rotating at 150 Hz, degassed in low vacuum, and toluene was evaporated in an air-circulating oven at 40 °C. Degassing and evaporation time was 30 min each. Cube samples with MWCNT concentrations up to 2.0 wt % were manufactured by solution casting into SU-8 coated aluminum molds, followed by thermal curing in an air-circulating oven. The fractional variability in MWCNT concentration was estimated at ±0.1. The cube edges were 10 mm in length.

5.2. Electromechanical Characterization. Uniaxial compression was applied using an electromechanical testing system (MTS Insight 5, MTS Systems Corp.), and the electrical resistance was obtained simultaneously using a high resistance meter (Model 6517A, Keithley Instruments Inc.). The cube samples were contacted on opposite sides with gold-coated silicon wafer electrodes that were contacted by kapton insulated silver plated copper wires using conductive silver paint. The applied compressive load and electric current were in parallel; i.e., the load was applied onto the electrodes. For improved electrical contact between the material and the electrodes, a 0.11 prestrain was applied. The applied compressive strain rate was 0.05 min^{-1}, and the DC voltage was 10 V. All measurements were taken at room temperature. The electrical resistance was calculated from the applied voltage and the measured current, and the compressive strain was obtained by dividing the measured crosshead displacement of the electromechanical testing system by the initial edge length of the sample.

5.3. Electrical Characterization. The DC volume conductivity as a function of MWCNT content was evaluated on the cube samples at $\varepsilon_0 = 0.11$ and on thin film samples according to ASTM D257, using the high resistance meter and a resistivity test fixture (Model 8009, Keithley Instruments Inc.). Thin film samples with MWCNT concentrations up to 2.0 wt % were obtained by solution casting onto release film covered glass substrates, followed by thermal curing in an air-circulating oven. The samples were 10 cm in diameter and varied in thickness from 0.4 to 1 mm. The results from the two test methods were in good agreement.

5.4. Applying the Model to Data from the Literature. In case the electric response was given as a function of pressure, P, or compressive force, F_c, the corresponding compressive strain was assumed to follow the relation:

$$\varepsilon_c \approx \frac{P}{Y} = \frac{F_c}{A_0 Y} \tag{8}$$

where Y is the Young's modulus of the polymer nanocomposite and A_0 is the area onto which F_c was applied. The degree to which a polymer nanocomposite resists uniaxial compression or tension typically increases with increasing deformation; for elastomers and small deformations, however, this effect is small (cf. Figure 5 in ref 23), and we therefore believe that the above approximation is acceptable. Y values are specified in Tables 1 and 2.

AUTHOR INFORMATION

Corresponding Author

*Tel: +1 514 398 6303. E-mail: pascal.hubert@mcgill.ca.

Notes

The authors declare no competing financial interest.

ACKNOWLEDGMENTS

This work was supported in part by McGill University, through the McGill Engineering Doctoral Award program, and in part by the Canada Research Chair.

REFERENCES

(1) Malliaris, A.; Turner, D. T. *J. Appl. Phys.* **1971**, *42*, 614−618.

(2) Coleman, J. N.; Curran, S.; Dalton, A. B.; Davey, A. P.; McCarthy, B.; Blau, W.; Barklie, R. C. *Phys. Rev. B: Condens. Matter Mater. Phys.* **1998**, *58*, R7492−R7495.

(3) Knite, M.; Teteris, V.; Kiploka, A.; Kaupuzs, J. *Sens. Actuators, A* **2004**, *110*, 142−149.

(4) Thostenson, E. T.; Chou, T. W. *Adv. Mater.* **2006**, *18*, 2837−2841.
(5) Knite, M.; Tupureina, V.; Fuith, A.; Zavickis, J.; Teteris, V. *Mater. Sci. Eng., C* **2007**, *27*, 1125−1128.
(6) Zhang, R.; Baxendale, M.; Peijs, T. *Phys. Rev. B: Condens. Matter Mater. Phys.* **2007**, *76*, 195433.
(7) Park, M.; Kim, H.; Youngblood, J. P. *Nanotechnology* **2008**, *19*, 055705.
(8) Pham, G. T.; Park, Y. B.; Liang, Z.; Zhang, C.; Wang, B. *Composites, Part B* **2008**, *39*, 209−216.
(9) Kang, J. H.; Park, C.; Scholl, J. A.; Brazin, A. H.; Holloway, N. M.; High, J. W.; Lowther, S. E.; Harrison, J. S. *J. Polym. Sci., Part B: Polym. Phys.* **2009**, *47*, 994−1003.
(10) Wichmann, M. H. G.; Buschhorn, S. T.; Gehrmann, J.; Schulte, K. *Phys. Rev. B: Condens. Matter Mater. Phys.* **2009**, *80*, 245437.
(11) Lee, J. B.; Khang, D. Y. *Compos. Sci. Technol.* **2012**, *72*, 1257−1263.
(12) Nanni, F.; Mayoral, B. L.; Madau, F.; Montesperelli, G.; McNally, T. *Compos. Sci. Technol.* **2012**, *72*, 1140−1146.
(13) Zhao, J. H.; Dai, K.; Liu, C. G.; Zheng, G. Q.; Wang, B.; Liu, C. T.; Chen, J. B.; Shen, C. Y. *Composites, Part A* **2013**, *48*, 129−136.
(14) Yoshikawa, S.; Ota, T.; Newnham, R.; Amin, A. *J. Am. Ceram. Soc.* **1990**, *73*, 263−267.
(15) Zhang, X. W.; Pan, Y.; Zheng, Q.; Yi, X. S. *J. Polym. Sci., Part B: Polym. Phys.* **2000**, *38*, 2739−2749.
(16) Hussain, M.; Choa, Y. H.; Niihara, K. *Composites, Part A* **2001**, *32*, 1689−1696.
(17) Zhang, X. W.; Pan, Y.; Zheng, Q.; Yi, X. S. *Polym. Int.* **2001**, *50*, 229−236.
(18) Zhou, J. F.; Sony, Y. H.; Zheng, Q.; Wu, Q.; Zhang, M. Q. *Carbon* **2008**, *46*, 679−691.
(19) Negri, R. M.; Rodriguez, S. D.; Bernik, D. L.; Molina, F. V.; Pilosof, A.; Perez, O. *J. Appl. Phys.* **2010**, *107*, 113703.
(20) Aneli, J. N.; Zaikov, G. E.; Khananashvili, L. M. *J. Appl. Polym. Sci.* **1999**, *74*, 601−621.
(21) Das, N. C.; Chaki, T. K.; Khastgir, D. *Carbon* **2002**, *40*, 807−816.
(22) Jiang, M. J.; Dang, Z. M.; Xu, H. P. *Appl. Phys. Lett.* **2006**, *89*, 182902.
(23) Chen, L.; Chen, G. H.; Lu, L. *Adv. Funct. Mater.* **2007**, *17*, 898−904.
(24) Jiang, M. J.; Dang, Z. M.; Xu, H. P.; Yao, S. H.; Bai, J. *Appl. Phys. Lett.* **2007**, *91*, 072907.
(25) Dang, Z. M.; Jiang, M. J.; Xie, D.; Yao, S. H.; Zhang, L. Q.; Bai, J. *J. Appl. Phys.* **2008**, *104*, 024114.
(26) Hu, C. H.; Liu, C. H.; Chen, L. Z.; Peng, Y. C.; Fan, S. S. *Appl. Phys. Lett.* **2008**, *93*, 033108.
(27) Cattin, C.; Hubert, P. *Mater. Res. Soc. Symp. Proc.* **2012**, 1410.
(28) Hwang, J.; Jang, J.; Hong, K.; Kim, K. N.; Han, J. H.; Shin, K.; Park, C. E. *Carbon* **2011**, *49*, 106−110.
(29) Hou, Y.; Wang, D.; Zhang, X. M.; Zhao, H.; Zha, J. W.; Dang, Z. M. *J. Mater. Chem. C* **2013**, *1*, 515−521.
(30) Pang, C.; Lee, C.; Suh, K.-Y. *J. Appl. Polym. Sci.* **2013**, *130*, 1429−1441.
(31) Sichel, E. K.; Sheng, P.; Gittleman, J. I.; Bozowski, S. *Phys. Rev. B: Condens. Matter Mater. Phys.* **1981**, *24*, 6131−6134.
(32) Li, C.; Thostenson, E. T.; Chou, T. W. *Appl. Phys. Lett.* **2007**, *91*, 223114.
(33) Oliva-Aviles, A. I.; Aviles, F.; Seidel, G. D.; Sosa, V. *Composites, Part B* **2013**, *47*, 200−206.
(34) Balberg, I.; Anderson, C. H.; Alexander, S.; Wagner, N. *Phys. Rev. B: Condens. Matter Mater. Phys.* **1984**, *30*, 3933−3943.
(35) Bauhofer, W.; Kovacs, J. Z. *Compos. Sci. Technol.* **2009**, *69*, 1486−1498.
(36) Stauffer, D.; Aharony, A. *Introduction to percolation theory*; Taylor & Francis: London, 1992.
(37) Vionnet-Menot, S.; Grimaldi, C.; Maeder, T.; Strässler, S.; Ryser, P. *Phys. Rev. B: Condens. Matter Mater. Phys.* **2005**, *71*, 064201.
(38) Balberg, I. *Phys. Rev. Lett.* **1987**, *59*, 1305−1308.
(39) Balberg, I. *Phys. Rev. B: Condens. Matter Mater. Phys.* **1998**, *57*, 13351−13354.
(40) Grimaldi, C.; Balberg, I. *Phys. Rev. Lett.* **2006**, *96*, 066602.
(41) Johner, N.; Ryser, P.; Grimaldi, C.; Balberg, I. *Phys. Rev. B: Condens. Matter Mater. Phys.* **2007**, *75*, 104204.
(42) Johner, N.; Grimaldi, C.; Balberg, I.; Ryser, P. *Phys. Rev. B: Condens. Matter Mater. Phys.* **2008**, *77*, 174204.
(43) Scardaci, V.; Coull, R.; Lyons, P. E.; Rickard, D.; Coleman, J. N. *Small* **2011**, *7*, 2621−2628.
(44) Tonpheng, B.; Yu, J.; Andersson, B. M.; Andersson, O. *Macromolecules* **2010**, *43*, 7680−7688.